Poly(acrylonitrile) encapsulated graphite as anode materials for lithium ion batteries

Kunkun Guo, Qinmin Pan, Shibi Fang[*]

Institute of Chemistry, Chinese Academy of Sciences, Beijing 100080, PR China

Abstract

Novel surface modification approach for graphite anode of lithium ion batteries was developed in this study. Poly(acrylonitrile) was in situ encapsulated on the surface of natural graphite (N-graphite) particles via radiation-initiated polymerization. The graphite obtained shows a large improvement in electrochemical performance such as initial Coulombic efficiency and cycleability compared with the original N-graphite. The structural stability of graphite surface is enhanced due to the fact that encapsulated poly(acrylonitrile) can depress the co-intercalation of solvated lithium ion.
© 2002 Elsevier Science B.V. All rights reserved.

1. Introduction

Natural graphite (N-graphite) has been intensively researched as the anode material of lithium ion batteries because it exhibits high capacity, desirable discharge–charge curves. However, large irreversible capacity loss and poor cycling life have been persistent problems with the wide application of N-graphite anodes [1,2].

The problems are mainly caused by the high anisotropy of the graphite surface and the weak bonds (van der Waals forces) between the graphite layers. These structural characteristics result in profound difference in chemical and electrochemical reactivity of the basal plane and the edge plane of the graphite, which determines the heterogeneity and fragility of the solid electrolyte interface (SEI) film formed. It is well known that the nature of the SEI film plays a significant role in electrochemical performance of graphite anode [3–5]. Another problem related to these structural characteristics is the expansion and exfoliation of graphite layers caused by co-intercalation of solvated Li^+ during lithium intercalation [6]. The net consequence of these problems is that slight volume and surface changes of the graphite particle during lithium ion migration will cause breakdown and then repair of the SEI film formed on a small scale [1–6]. In order to control the irreversible capacity loss and enhance the cycling life of the N-graphite anode,

Aurbach et al. [7] had concluded that it is necessary to make the SEI film formed very compact and flexible.

Interests have been focused on the surface encapsulation of N-graphite particles with ionic conductive polymer in our group. The aim of our work is to form polymeric film on the surface of N-graphite particles, and the polymer is flexible enough to accommodate the slight volume and surface changes of the graphite particles, thus reducing irreversible capacity and enhancing cycleability of the N-graphite electrodes.

In this paper, poly(acrylonitrile) was in situ encapsulated on the surface of N-graphite particles through radiation-initiated polymerization technique and attention had been paid to the effect of poly(acrylonitrile) on the electrochemical properties of the modified graphite.

2. Experimental

The N-graphite powder used in this study was obtained from Nanshu Grphite Co. (Shangdong province, PR China) and was labeled as N-graphite. Scanning electron microscopy (SEM, S-530, Hitachi) was employed to investigate the surface morphology of the N-graphite.

Polymerization of acrylonitrile was conducted using a cobalt 60 γ-ray source in a radiation tube as described in the following procedure. N-graphite powder and a given amount of acrylonitrile monomer (100:1.50, w/w) were added to dry methanol and vigorous stirred. The mixture was then

* Corresponding author. Fax: +86-10-62559373.
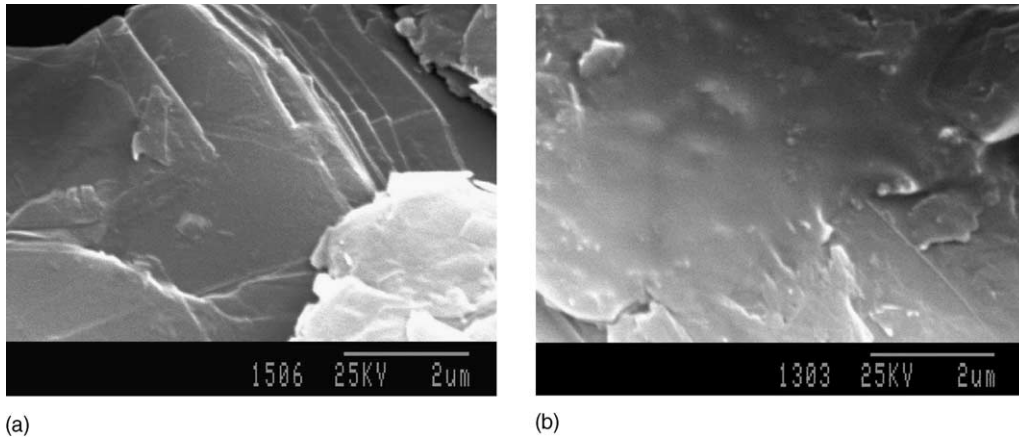*E-mail address:* fangsb@infoc3.icas.ac.cn (S. Fang).

Fig. 1. Scanning electron microscope images of the natural graphite sample before and after encapsulation of poly(acrylonitrile): (a) natural graphite; (b) encapsulated graphite.
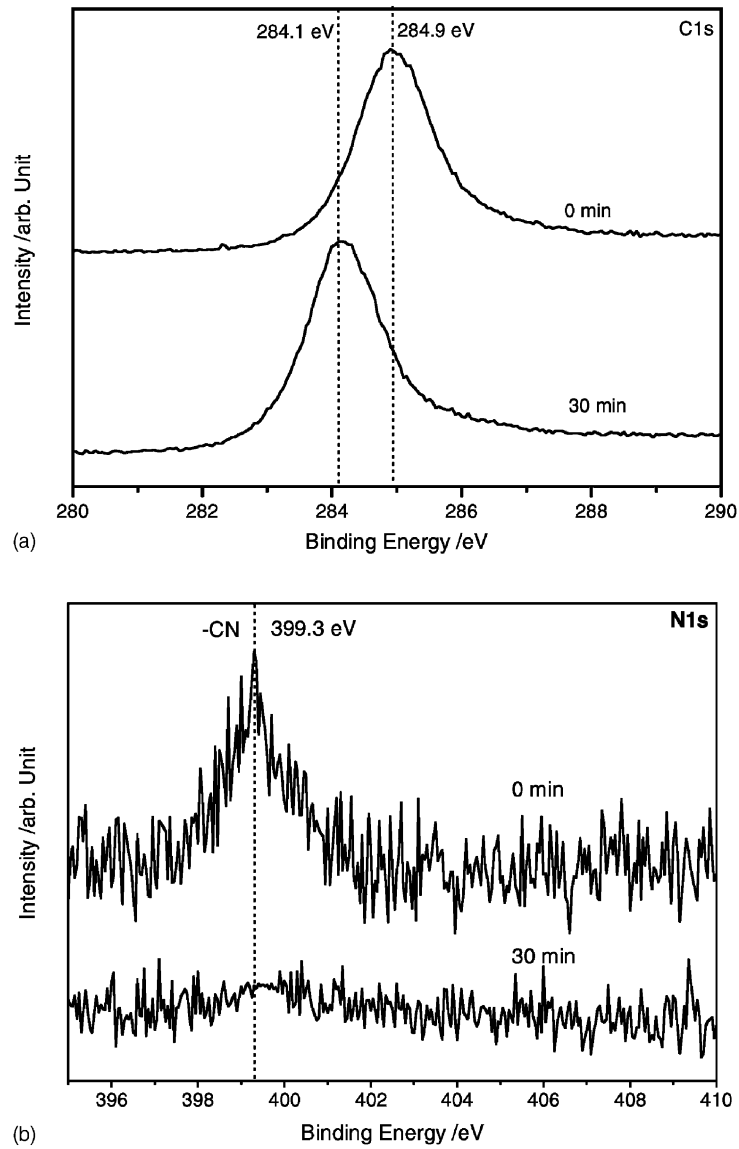

Fig. 2. X-ray photoelectron spectra for carbon C 1s, N 1s in the encapsulated graphite samples before and after 30 min sputtering, sputtering rate: 20 Å min^{-1}, (a) C 1s; (b) N 1s.
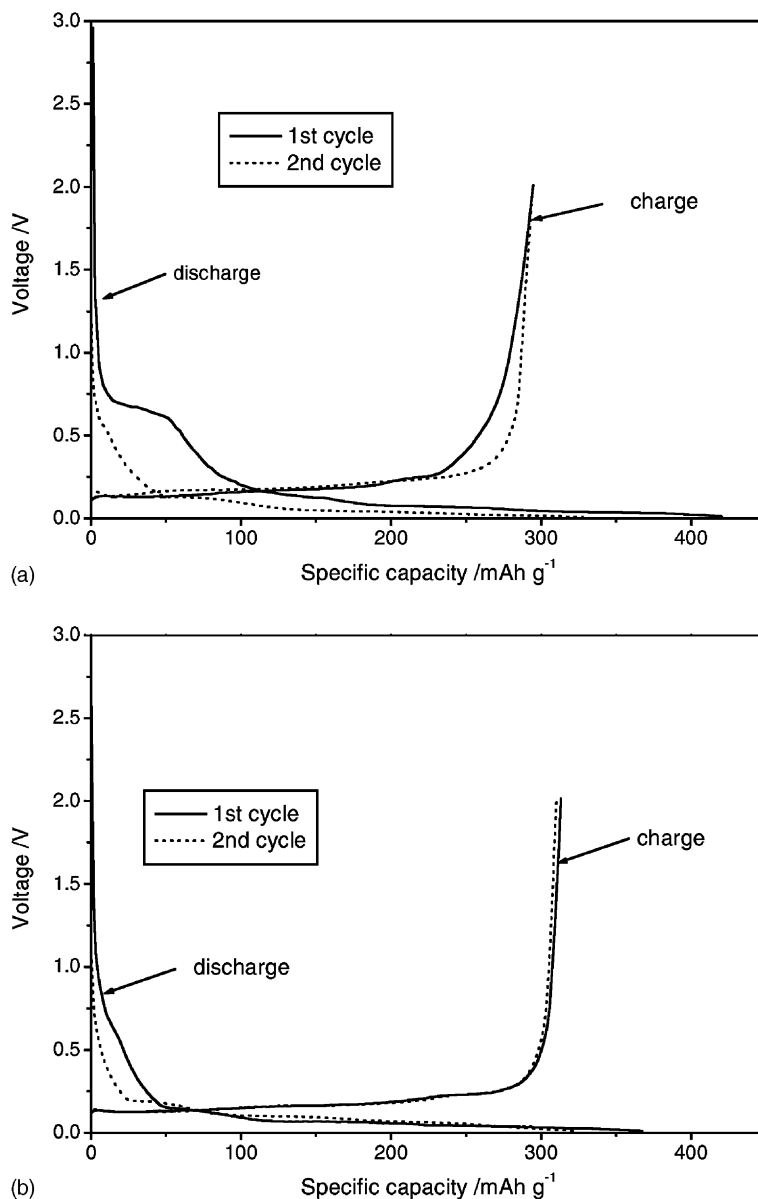
Fig. 3. Discharge–charge profiles of the natural and encapsulated graphite electrodes in the PC-based electrolyte, current density: 0.20 mA cm^{-2}; (a) natural graphite; (b) encapsulated graphite.

transferred to a radiation tube filled with N_2 and held under a cobalt 60 γ-ray source, and polymerization reaction was allowed to take place until a radiation dose of 4 million rad had been reached. After reaction, the mixture was filtered and no free monomers were detected, the resultant graphite was rinsed with methanol and dried. The graphite powder obtained was called encapsulated graphite (E-graphite).

X-ray photoelectron spectroscopy (XPS; ESCALAB2020I-XL) measurements were performed in a ultrahigh vacuum (UHV; 2.5×10^{-10} Torr base pressure) with the use of a monochromatic Al Kα source (1486.6 eV). The depth profiles were obtained by argon ion sputtering (4 kV), at a sputtering rate of 20 Å min^{-1} on a SiO_2–Si sample to determine the thickness of the encapsulated polymer film.

Raman spectra were excited by using a 514.5 nm line (50 mW) of an argon ion laser (NEC, GLG3260), and then were recorded using a Raman spectrometer (Jobin-Yvon T-64000) equipped with a multichannel charge-coupled device (CCD) detector.

Preparation of graphite electrodes and the assembly of cells were described elsewhere [1–4]. The electrolyte used was 1 mol l^{-1} LiPF$_6$ solution in a 1:1:1 (v/v/v) mixture of ethylene carbonate (EC), diethylene carbonate (DEC) and propylene carbonate (PC). The cells were discharged and charged between 0.010 and 2.000 V versus Li/Li$^+$ at a constant current density of 0.20 mA cm^{-2} using a computer-controlled battery tester. Cyclic voltammograms (CV) were obtained using three-electrode cells at a scan rate of 0.2 mV s^{-1}.
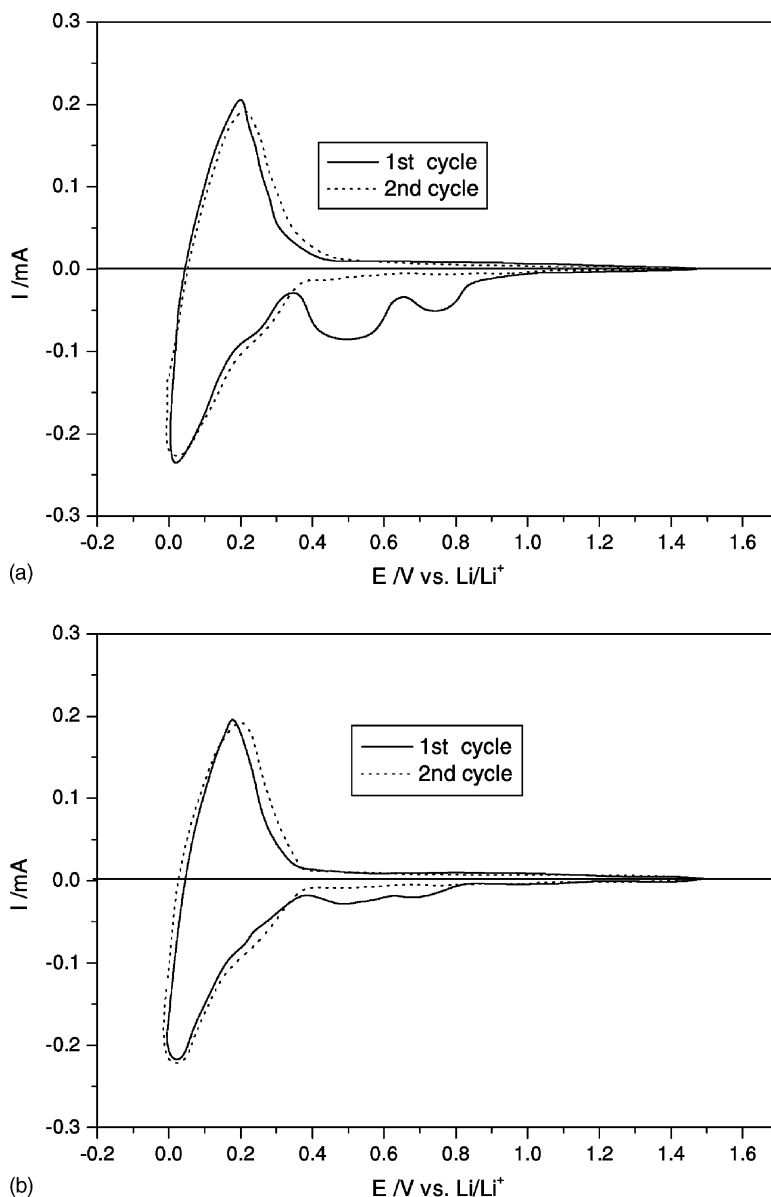
Fig. 4. Cycle voltammograms of the natural and encapsulated graphite electrodes in the PC-based electrolyte: (a) natural graphite; (b) encapsulated graphite.

Electrochemical impedance measurements were carried out using IM6e impedance analyzer (Zahner Electrik). Impedance spectra were potentiostatically measured by applying an ac voltage of 10 mV amplitude over the frequency range from 10 kHz to 10 mHz after the electrode had attained an equilibrium at each potential. All the potentials indicated here were referred to the Li/Li$^+$ electrode potential.

3. Results and discussion

3.1. Characterization of the encapsulated graphite

Fig. 1 shows the scanning electron microscope (SEM) images of the N-graphite and poly(acrylonitrile) E-graphite samples. The surface of N-graphite displays a glossy and bare morphology, whereas the surface of the E-graphite particles looks rough and is evidently covered by thin film. However, this thin film has been only encapsulated on the partial surface of N-graphite, and inclines to coat the edge sites with more reactive [5].

Fig. 2 shows the XPS depth profiles of the E-graphite sample before and after 30 min of argon ion sputtering at a rate of 20 Å min^{-1}. Clearly, the C 1s peaks for C–C in polymer (284.9 eV) and N 1s peak for C≡N (399.3 eV) which assigned to the poly(acrylonitrile) are observed at 0 min. After 30 min etching, the N 1s peak disappears and the C 1s peak (284.1 eV) that assigned to the N-graphite appears [8–10]. The SEM images and XPS spectra demonstrate that the poly(acrylonitrile) has been coated on the
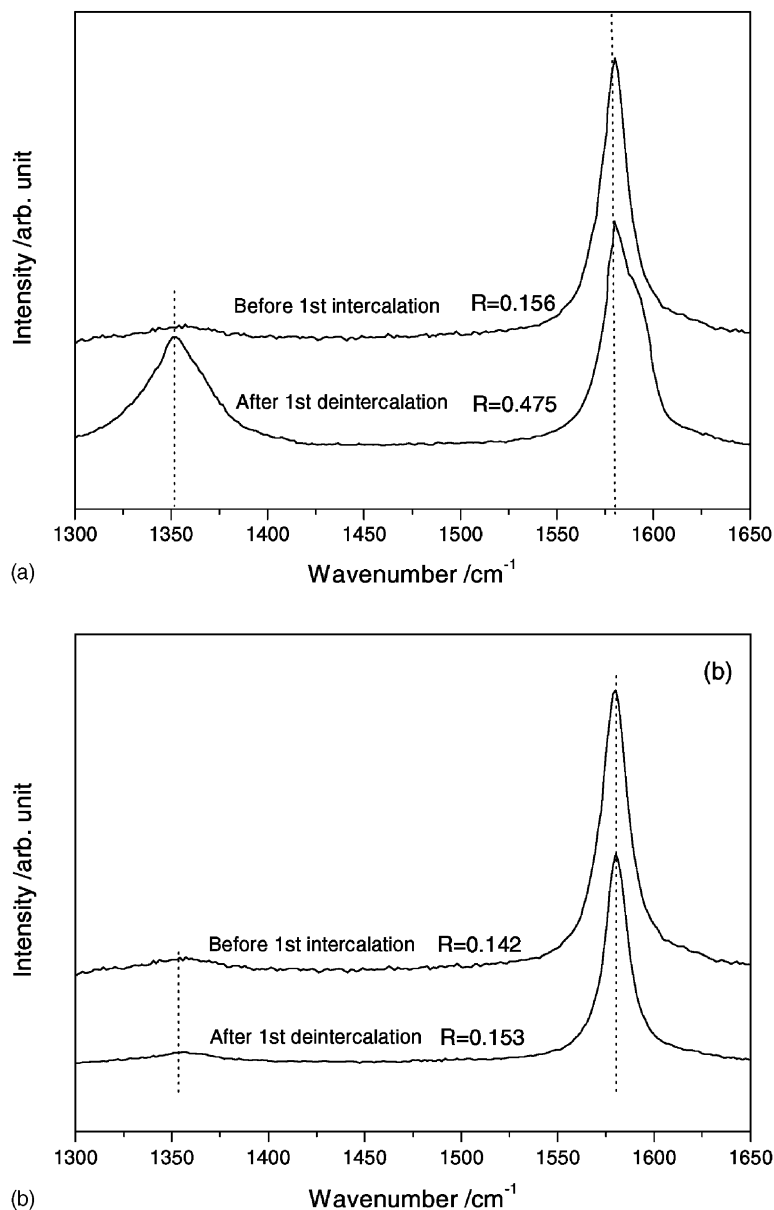
Fig. 5. Raman spectra of the natural and encapsulated graphite electrodes before and after first cycle: (a) natural graphite electrode; (b) encapsulated graphite electrode.

surface of the E-graphite with a thickness of about 60 nanometers.

3.2. Discharge–charge properties of the encapsulated graphite

The typical discharge–charge (intercalation/de-intercalation) profiles of the N-graphite and E-graphite electrodes are shown in Fig. 3. A plateau at about 0.75 V in the first discharge curve, which ascribed to electrolyte decomposition and SEI film formation [2,3], is observed for N-graphite electrode (seen in Fig. 3a), whereas that of the E-graphite electrode (seen in Fig. 3b) becomes much smaller. Accordingly, the irreversible capacity consumed on the formation of

SEI film for E-graphite electrode is expected to be lower due to the fact that poly(acrylonitrile) cover some edge sites prone to electrolyte decomposition [3].

CV of the N-graphite and E-graphite electrodes are presented in Fig. 4. Two cathodic (reduction) peaks in the potential range of 0.6–0.9 V and 0.3–0.6 V are observed for the N-graphite in the first cycle, and these peaks disappear during the second cycle (seen in Fig. 4a). These peaks are attributed to the SEI film formation (0.6–0.9 V) and co-intercalation of solvated Li^+ (0.3–0.6 V), respectively [11,12]. These peaks decrease dramatically after encapsulation by poly(acrylonitrile) (seen in Fig. 4b), and no difference can be found in the anodic peaks (de-intercalation process) between two graphite electrodes. These results
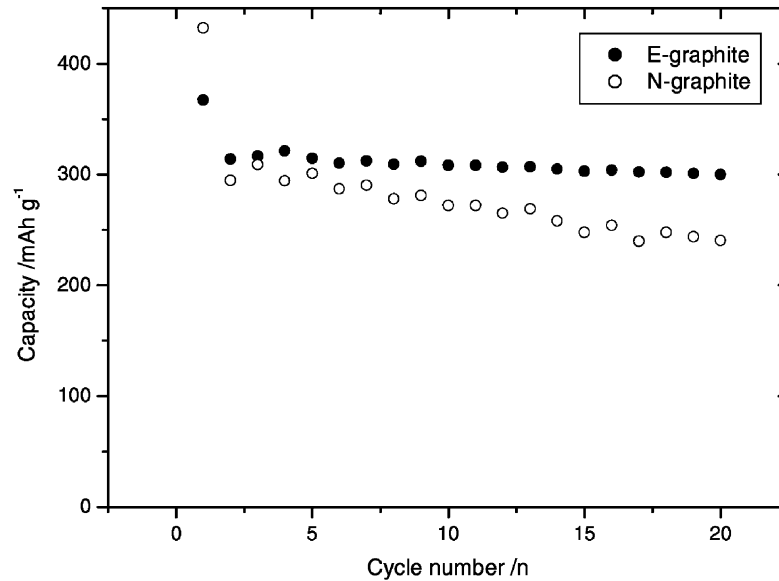
Fig. 6. Cycling characteristics of the natural and encapsulate graphite electrodes at a current density of 0.2 mA cm^{-2} in the PC-based electrolyte.

indicate that encapsulation of poly(acrylonitrile) on the N-graphite surface can depress the irreversible capacity caused by formation of the SEI film and co-intercalation of solvated Li^{+}.

3.3. Raman spectroscopy study

Fig. 5 displays Raman spectra of the two graphite electrodes before and after the first discharge–charge cycle. As shown in Fig. 5, an asymmetric E$_{2g2}$ band at 1580 cm^{-1} with a weak shoulder is observed and a new band at 1352 cm^{-1} appears for N-graphite electrode after the first cycle compared to the original N-graphite (seen in Fig. 5a). These results indicate that the structure of the N-graphite surface were somewhat damaged and could not be returned to the

original structure [13]. This conclusion can also be supported by the appearance of the peak at 1352 cm^{-1} and variation of the R (the ratio of peak intensity in 1352 cm^{-1} to that at 1580 cm^{-1}, e.g. I_{1352}/I_{1580}) value in Fig. 5. The peak at 1352 cm^{-1} corresponds with the disordered structure of N-graphite and the R-value is proportional to degree of surface disorder [13,14]. Increase in the R-value and appearance of 1352 cm^{-1} band indicate increasing in surface disorder and amorphization of the graphite surface. On the contrary, the E$_{2g}$ bands of the E-graphite electrode exhibit no difference in peak intensity, bandwidth and R-value before intercalation and after de-intercalation (seen in Fig. 5b). Raman spectra makes it clear that encapsulation of flexible and stretch poly(acrylonitrile) on the N-graphite can accommodate the expansion of graphite layers and
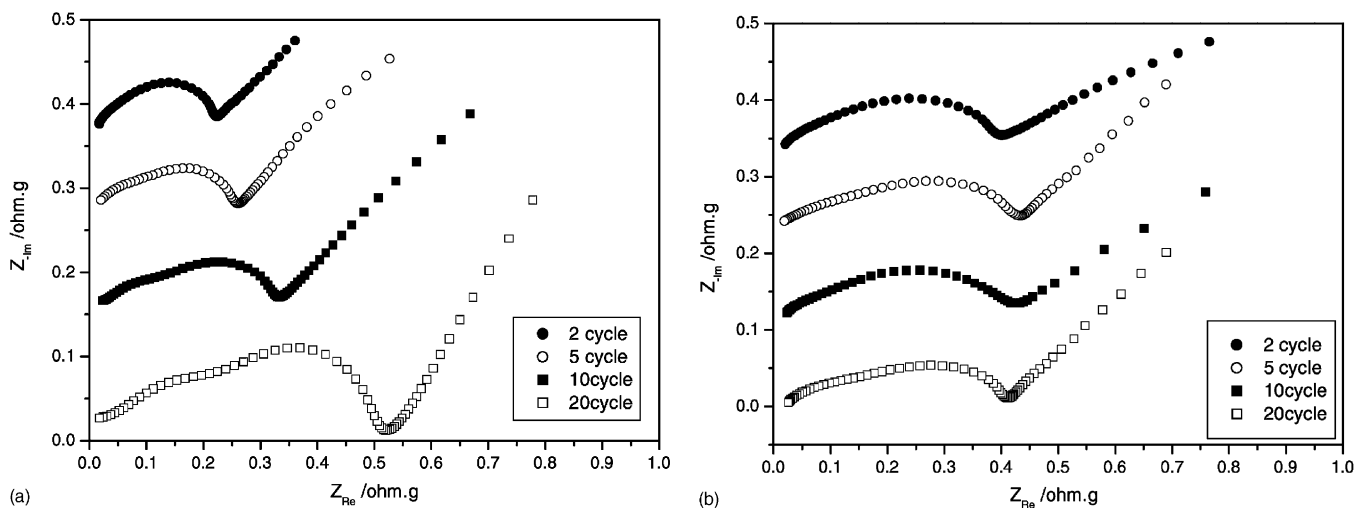

Fig. 7. Electrochemical impedance spectra of the natural and encapsulated graphite electrodes after difference cycling numbers: (a) natural graphite; (b) encapsulated graphite.

resist the destruction of graphite surface caused by the co-intercalation of solvated Li$^+$ during the Li intercalation process.

3.4. Cycling characteristics of the encapsulated graphite

Discharge–charge cycling performances of the E-graphite and N-graphite electrodes in PC-based electrolyte are illustrated in Fig. 6. The E-graphite electrode exhibits stable capacity and shows smaller capacity fading than that of the N-graphite upon prolonged cycling.

Fig. 7 shows the impedance spectra of the E-graphite and N-graphite electrodes at 0.20 V versus Li/Li$^+$ (discharge process) after different cycling numbers. Depressed semicircles in the high and middle frequency regions are observed for both electrodes as seen in Fig. 7. As has been reported previously [15–18], the semicircles in high and middle frequency regions were due to Li ion migration through the SEI film and the charge-transfer reaction at the interface between graphite and the SEI film, respectively. Upon cycling, the semicircles of the N-graphite electrode enlarged appreciably (seen in Fig. 7a), while the semicircle size of the E-graphite electrode almost remains unchanged (seen in Fig. 7b). Enlarging of the high-frequency semicircle implied thickening of the SEI film after repeated cycling. This can be explained by the fact that exfoliation of the graphene layers caused by the co-intercalation of solvated lithium ion will leads to breakdown and additional growth of the SEI film on a small scale [7]. In contrast, additional growth of the SEI film of the E-graphite electrode can be avoided during the repeated cycling, as reflected by the constant impedance in Fig. 7b. Therefore, one mechanism for capacity fading is considered to be the pronounced increase in electrode's impedance upon cycling, which ascribes to thickening of the SEI film and then electrical disconnection of the graphite particles, could be avoided for the E-graphite electrode.

4. Conclusion

Based on the above results, encapsulation of poly(acrylonitrile) on the surface of N-graphite cannot only depress the irreversible capacity caused by co-intercalation of sol-vated Li$^+$ and exfoliation of the graphite layers, but also avoid markedly increasing in electrode's impedance. Encapsulation of poly(acrylonitrile) contributes to the stability of the graphite particles surface during cycling. As a result, the E-graphite electrodes show a large improvement in initial Coulombic efficiency and cycleability in PC-based electrolyte.

References

[1] P. Arora, R.E. White, J. Electrochem. Soc. 145 (10) (1998) 3647.
[2] K. Tatsumi, N. Iwashita, H. Sakaebe, H. Shioyama, J. Electrochem. Soc. 142 (3) (1995) 716.
[3] G.C. Chung, S.H. Jun, K.Y. Lee, M.H. Kim, J. Electrochem. Soc. 146 (5) (1999) 1664.
[4] K. Suzuki, T. Hamada, T. Sugiura, J. Electrochem. Soc. 146 (3) (1999) 890.
[5] G.C. Chung, H.J. Kim, S.H. Yu, S.H. Jun et al., J. Electrochem. Soc. 147 (12) (2000) 4391.
[6] H. Shi, J. Barker, M.Y. Saidi, R. Koksbang, J. Electrochem. Soc. 143 (11) (1996) 3466.
[7] D. Aurbach, B. Markovsky, M.D. Levi, E. Levi, A. Schechter, J. Power Sources 81/82 (1999) 95.
[8] D. Bar-Tow, E. Peled, L. Burstein, J. Electrochem. Soc. 146 (3) (1999) 824.
[9] Y.P. Wu, S.B. Fang, Y.Y. Jiang, Solid State Ionics 120 (1999) 117.
[10] T. Sotomura, K. Adachi, M. Taguchi, M. Iwaku et al., J. Power Sources 81/82 (1999) 192.
[11] P. Yu, B.S. Haran, J.A. Ritter, R.E. White, B.N. Popov, J. Power Sources 91 (2000) 107.
[12] M. Yoshio, H.Y. Wand, K. Fukuda, Y. Hara, Y. Adachi, J. Electrochem. Soc. 147 (4) (2000) 1245.
[13] P. Novak, F. Joho, R. Imhof, J.C. Panitz, O. Haas, J. Power Sources 81/82 (1999) 212.
[14] M. Inaba, H. Yoshida, Z. Ogumi, T. Abe et al., J. Electrochem. Soc. 142 (1) (1995) 20.
[15] W.W. Huang, R. Frech, J. Electrochem. Soc. 145 (3) (1998) 765.
[16] E. Barsoukov, J.H. Kim, C.O. Yoon, H. Lee, Solid State Ionics 116 (1999) 249.
[17] Y.C. Chang, H.J. Sohn, J. Electrochem. Soc. 147 (1) (2000) 50.
[18] Q.M. Pan, K.K. Guo, S.B. Fang, J. Mater. Chem. 12 (2002) 1833.